

Received March 6, 2019, accepted April 1, 2019, date of publication April 9, 2019, date of current version April 19, 2019.

Digital Object Identifier 10.1109/ACCESS.2019.2909847

An Alternative to IEEE 802.11ba: Wake-Up Radio With Legacy IEEE 802.11 Transmitters

MARTÍ CERVIA CABALLÉ^{ID1}, ANNA CALVERAS AUGÉ^{ID1}, ELENA LOPEZ-AGUILERA^{ID1}, EDUARD GARCIA-VILLEGAS^{ID1}, ILKER DEMIRKOL^{ID1}, AND JOSEP PARADELLS ASPAS^{1,2}

¹Department of Network Engineering, Universitat Politècnica de Catalunya (UPC), 08034 Barcelona, Spain

²I2cat Foundation, 08034 Barcelona, Spain

Corresponding author: Martí Cervià Caballé (marti.cervia@upc.edu)

This work was supported in part by the ERDF and the Spanish Government through project TEC2016-79988-P, AEI/FEDER, UE and by the Secretaria d'Universitats i Recerca del Departament d'Empresa i Coneixement de la Generalitat de Catalunya 2017 SGR 376.

ABSTRACT Current standardization process for Wake-up Radio (WuR) within the IEEE 802.11 Working Group, known as the IEEE 802.11ba, has brought interest to the IEEE 802.11-related technologies for the implementation of WuR systems. This paper proposes a new WuR system, where the Wake-up Transmitter (WuTx) is based on the legacy IEEE 802.11 Orthogonal Frequency Division Modulation (OFDM) Physical Layer (PHY) specification. Using the IEEE 802.11, OFDM PHY makes it possible for an IEEE 802.11a/g/n/ac transmitter to operate as WuTx for this WuR system. The WuTx generates a Wake-up Signal (WuS) coded with an amplitude-based digital modulation, achieving a bit rate of 250 kbps. This modulation, which we call Peak-Flat modulation, can be received using low-power receivers. A simulated proof of concept of the WuTx based on the IEEE 802.11g is presented and evaluated using MATLAB WLAN Toolbox. A method to generate the Peak-Flat modulated WuS from an IEEE 802.11a/g standard-compliant transmitter, using only software-level access, is explained. In addition, two possible low-power Wake-up Receiver (WuRx) architectures capable of decoding the presented modulation are proposed. The design of those receivers is generic enough to be used as a reference to compare the performance of the Peak-Flat Modulation with the other state-of-the-art approaches. The evaluation results conclude that the Peak-Flat modulation has similar performance compared to the other IEEE 802.11 WuR solutions on the reference receivers. Moreover, this solution provides a notorious advantage: legacy OFDM-based IEEE 802.11 transmitters can generate the Peak-Flat modulated WuS.

INDEX TERMS WLAN, IEEE 802.11, IEEE 802.11ba, Wake-up Radio, WSN, energy-efficient communication.

I. INTRODUCTION

Devices compliant with the IEEE 802.11 family of specifications are pervasive, with over 9.5 billion installed devices, as of 2018 [1]. Infrastructure for IEEE 802.11 devices is also extensive, with 50 million Wi-Fi networks in the US alone [2]. With this adoption rate, IEEE 802.11 could become a suitable solution for many Internet of Things (IoT) applications [3]. However, the power consumption of IEEE 802.11 devices is too high for most IoT based use cases, where the devices are energy constrained, powered through either

The associate editor coordinating the review of this manuscript and approving it for publication was Nitin Nitin.

batteries or power harvesting. The current solution to this issue is IEEE 802.11 Power Saving Mode (PSM), which was presented in its original specification and improved in subsequent IEEE 802.11 releases. PSM periodically toggles the device radio, keeping it off most of the time, in order to reduce energy expenditure. The length of the off periods ranges from several beacon intervals (in the original IEEE 802.11 specification), up to several years (using IEEE 802.11ah [3]). To avoid losing frames sent to sleeping stations, the Access Point (AP) of the network stores any frame directed to a sleeping station (STA). These stored frames are fetched by the STA at the time of its scheduled wake-up. Indeed, PSM is effective in reducing idle listening time but

its use introduces latency, as communication with an STA has to wait for its next scheduled wake-up. Consequently, PSM suffers from a trade-off between a reduction in power consumption through long sleep cycles, and the increase in latency that these introduce. Thus, PSM is not efficient for traffic profiles that require low-latency, as those consisting of short but frequent frame transmissions [4].

Aiming to get a solution for IEEE 802.11, which can be both low-latency and low-power, the Wake-up Radio (WuR) concept (see Section II) is proposed. With WuR, the main radio of the device is kept off and is only activated to receive incoming transmissions. For this purpose, a WuR enabled device uses the secondary radio receiver, usually referred to as Wake-up Receiver (WuRx), to receive asynchronous wake-up requests from other devices. These requests, called WuS (Wake-up Signals), are generated by other devices on the network using their main (or secondary) transmitters as Wake-up Transmitters (WuTx). The power consumption of the WuRx must be low enough to allow for its continuous operation. Hence, WuR does not suffer from any efficiency vs. latency trade-off since the sleeping stations can be woken up on-demand. Moreover, WuR presents lower energy consumption than some of the most used duty-cycling schemes, as shown in the literature [5], [6].

Due to the growing interest on WuR, IEEE started standardization efforts with the aim of incorporating it into the IEEE 802.11 specification. This standardization process is, at the moment of writing, under development for the forthcoming IEEE 802.11ba specification [7]. One of the defining characteristics of IEEE 802.11ba is its use of the IEEE 802.11 radio as WuTx. IEEE 802.11ba, like most other WuR systems [8], transmits a WuS coded using On-Off Keying (OOK). In contrast to the signaling schemes used by prior IEEE 802.11 specifications, OOK is an amplitude-based modulation that can be received with feature-limited, low-power WuRx. OOK uses two amplitude levels as symbols: the first symbol presents a low amplitude, as close as possible to zero, representing the “0” logic value, the second symbol presents a constant high amplitude level, representing the “1” logic value. However, none of the Physical Layers (PHY) specified in the current IEEE 802.11 specification supports the transmission of symbols with low constant amplitude, and, as a consequence, legacy IEEE 802.11 devices are unable to transmit the low amplitude OOK symbol with fidelity. Consequently, IEEE 802.11ba proposes a modified version of the 802.11 Orthogonal Frequency Division Modulation (OFDM) PHY transmitter that is capable of transmitting waveforms with close to zero amplitude, thus, allowing for reliable OOK symbol transmission.

As a result of these modifications, the transmitters of existing, and already deployed IEEE 802.11 devices are incompatible with the new specification, since they cannot generate the WuS defined by IEEE 802.11ba. However, keeping backward compatibility with legacy transmitters is necessary for interoperability between legacy IEEE 802.11 devices and the

new IEEE 802.11ba enabled devices. For example, without backward compatibility, a legacy device is not able to interact directly with a sleeping IEEE 802.11ba device since it cannot send the WuS required for its wake-up.

A. LEGACY COMPATIBLE WUR

The work presented in this paper is a WuR solution alternative to IEEE 802.11ba, which features a backward compatible WuTx based on the legacy IEEE 802.11 OFDM PHY specification. Our solution uses the legacy IEEE 802.11 OFDM PHY transmitter as WuTx. In order to maintain backward compatibility, it uses an amplitude-based modulation that differs from OOK, which we will call Peak-Flat modulation. Peak-Flat modulation achieves a bit rate of 250 kbps and can be received using low-power non-coherent receivers, such as envelope detectors. It is composed of two different symbols, a Peak Symbol that presents a very high peak and a Flat Symbol, with a flatter and smoother profile. Peak-Flat encapsulates the WuS in a standard compliant IEEE 802.11 frame and uses the standard IEEE 802.11 Media Access Control (MAC) to ensure compatibility with current WLAN technologies.

Additionally, we propose a software-based method to generate the waveforms for the Peak-Flat modulation on a standard IEEE 802.11g transmitter. The method proposed requires that the scrambling sequence generated by the IEEE 802.11 transceiver is known beforehand. Access to this information is not enabled in most of the current IEEE 802.11 commercial driver stacks. However, we believe that this novel use case can drive the manufacturers’ interest to either document their scrambler seed generation processes or to update the drivers and firmware of their IEEE 802.11 products to expose this information. The aforementioned method is also directly compatible with other OFDM based IEEE 802.11 PHY, such as IEEE 802.11a. Moreover, it can also be applied with minor modifications to IEEE 802.11n/ac, as discussed in Section VII-A. Our proposal is designed as an alternative to IEEE 802.11ba, nonetheless, interoperability between our solution and the future IEEE 802.11ba is discussed in Section IX.

A Proof of Concept (PoC) implementation of the WuTx based on the proposed method is evaluated by means of simulation using MATLAB WLAN Toolbox, which provides simulation functions compliant with the IEEE 802.11 standard [9]. We propose two possible low-power WuRx architectures capable of decoding the Peak-Flat modulation. Both architectures serve as demonstrators to check the feasibility of Peak-Flat modulation. One of them is a basic OOK receiver and the other is based on a peak detector. Finally, we present a PoC for the transmission of Peak-Flat modulation using simulations on both MATLAB WLAN Toolbox and Simulink [10]. The performance of this PoC is evaluated in AWGN and fading channels (IEEE 802.11 TGn Channel B). To put in context the performance of Peak-Flat modulation proposed in this WuR system, we evaluate other state-of-the-art modulations used in WuR with simulated

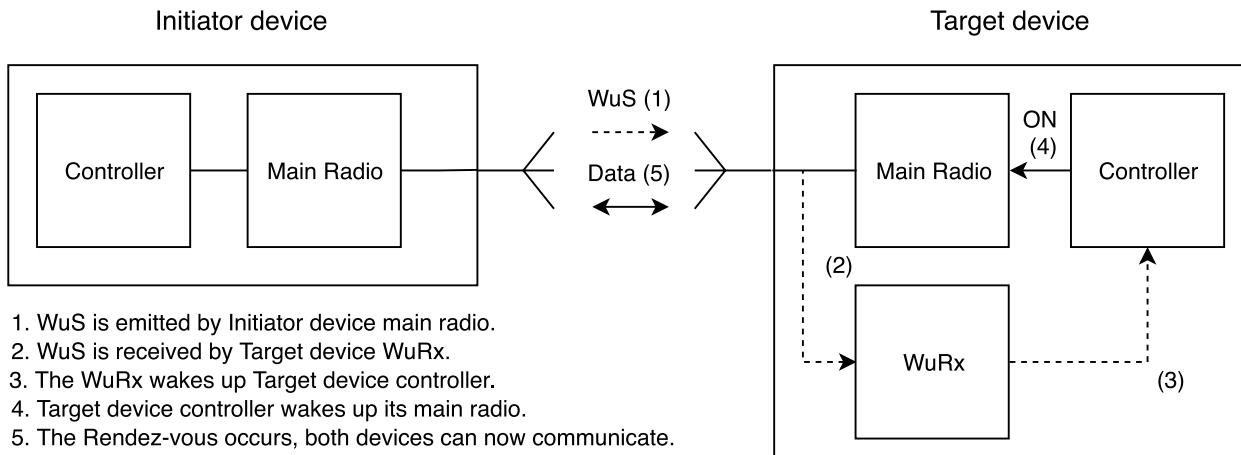


FIGURE 1. Diagram explaining the operation of a WuR system, where the main radio is also the WuTx.

implementations of the proposed WuRx architectures: an OOK modulation with $4\ \mu s$ pulses and a Manchester encoded OOK modulation with $2\ \mu s$ pulses, equivalent to IEEE 802.11ba's fast data rate. The OOK receiver implemented on the PoC is used as the reference receiver for the evaluation.

The remainder of this paper is structured as follows. Section II introduces the WuR concept. Section III exposes the state of the art of WuR using IEEE 802.11 technologies. Section IV presents the structure of IEEE 802.11 PHY and the Peak-Flat modulation as an alternative to OOK. Sections V and VI explain the generation of Peak-Flat symbols using an IEEE 802.11g transmitter. Section VII proposes a WuS generation method for IEEE 802.11g. Section VIII describes and compares the two possible WuRx architectures. Section IX develops the topic of compatibility between the proposed WuR system and IEEE 802.11ba. Finally, Section X presents the conclusions and future work.

II. WAKE-UP RADIO SYSTEMS

WuR is one of the many MAC based techniques used to reduce the power consumption of wireless communication devices. These techniques maintain the device radio powered off most of the time. It is only activated when a message needs to be transmitted or received. Doing so reduces the duty cycle of the device radio and, as a consequence, minimizes power consumption. However, there is a need for a coordination mechanism for such a scheme to function. Devices need to toggle their radios in a coordinated manner to maintain communications among them. Such a mechanism is referred to as *rendez-vous* scheme and determines the method used to coordinate the wake-up of devices in the network.

Three categories of *rendez-vous* schemes are listed in [11]:

- Purely synchronous:

Nodes are synchronized to wake up at a certain time interval. Additional protocol overhead is usually required to maintain the synchronization as well as low drift clocks, which are not available on

feature-limited nodes. One example of this category would be PSM mode of IEEE 802.11, where a sleeping STA has a *rendez-vous* with its AP after a pre-defined number of beacon intervals.

- Purely Asynchronous:

Nodes can wake up other nodes on demand. This scheme requires additional hardware (i.e., a secondary, low-power radio) to receive the wake-up requests from other devices. The current WuR implementation of IEEE 802.11ba is an example of a system implementing this scheme. Stations compatible with IEEE 802.11ba use a low-power secondary radio to receive wake-up requests from other IEEE 802.11ba devices.

- Pseudo-asynchronous:

Nodes wake up periodically but not synchronously. A node can wake up another node on demand by opportunistically synchronizing a transmission with the wake-up cycle of the other node. This scheme consumes additional power due to the multiple retransmissions required. One example of this scheme is Contikimac [12], which uses an opportunistic synchronization mechanism.

WuR is an implementation of a purely asynchronous *rendez-vous* scheme. In WuR systems, devices turn off their main radio but keep a low-power secondary radio continuously active. A diagram of a WuR *rendez-vous* is shown in Fig.1. The *rendez-vous* on WuR occurs in the following manner: 1. the Initiator device uses its WuTx to send a WuS to the Target device; 2. the Target device receives the WuS with its WuRx; 3. the Target device WuRx wakes up its controller from sleep; 4. the Target device controller activates its main radio; finally, 5. the main radios of both devices are active and the *rendez-vous* has occurred. In order for this scheme to work, the power consumption of the secondary radio must be low, in the order of several μW . Therefore, WuR requires a modulation that can be decoded using the lowest-power hardware possible. A recurring approach discussed widely in

the related literature for WuR is the use of signals that encode data using only amplitude, which can be decoded with mostly passive receiver designs [8]. These amplitude-based waveforms can be used to create simple digital modulations such as OOK, which is prominent in the literature [8]. OOK is the modulation chosen for all the state-of-the-art WuR systems powered by IEEE 802.11 presented in the next section.

III. IEEE 802.11 STANDARDS AND WAKE-UP RADIO

A. STATE-OF-THE-ART

To the best of our knowledge, there are three WuR solutions concerning IEEE 802.11 WuTx presented in the literature [13]–[15]. Additionally, we can count the WuR system still under development within TGba, IEEE 802.11ba. In relation to how they use IEEE 802.11 signals to generate the symbols that form the WuS, they can be classified into two categories: systems that use sequences of standard IEEE 802.11 frames to generate the WuS; and systems that encode the WuS symbols by using IEEE 802.11 OFDM PHY symbols.

The first type of systems uses IEEE 802.11 frames or frame sequences as symbols. These systems send, at most, one symbol per IEEE 802.11 frame. On the WuR systems studied, the information is encoded using the length [15] or the presence of IEEE 802.11 frames [14]. The WuTx for these systems can be implemented using only software. This can be achieved by using either a low-level Application Programming Interface (API) provided by the device or with the socket API provided by most operating systems. Both options provide a way to send raw IEEE 802.11 frames with arbitrary length and, in most cases, on arbitrary intervals. An example of this type of systems is the one presented in [14], which generates an OOK signal modulated with a synthetic 15 kHz carrier. This carrier is created by sending IEEE 802.11 frames at a 15 kHz rate. The presence of this carrier is required by the low-power Bit Decoder used to decode the signal, an AS3933 [16]. The system achieves a 1 kbps data rate. Another system that uses IEEE 802.11 at frame level is the one devised in [15]. The WuTx encodes binary data using the length of IEEE 802.11 frames, which is then decoded by an envelope detector and a counter circuit. The main drawback of this type of systems is that, as they operate at the frame level, their achievable bit rate is low, since it is limited by the frame rate of the IEEE 802.11 transmitter.

The second type of IEEE 802.11 WuR devices encodes binary data using the OFDM symbols of IEEE 802.11 OFDM PHY. On one hand, systems of this type can achieve higher data rates than the former. The symbol rate for IEEE OFDM PHY is 250 kBd using the most widely supported symbol period of 4 μ s. Consequently, the maximum achievable bit rate for this type of systems is a multiple of 250 kbps, depending on the number of bits per symbol. On the other hand, these systems are more complex to implement since they need to manipulate the waveforms generated by the OFDM symbols in order to create a signal recoverable by relatively simple WuRx. IEEE 802.11 PHY specifications

describe a complex transceiver architecture that incorporates: scrambling, coding, interleaving, pilot tone addition, guard intervals and other mechanisms added to increase performance and reliability. The effect of all these mechanisms on the output waveform must be also taken into account in the design of such a system. A system using IEEE 802.11 OFDM PHY to produce an imperfect OOK modulation is described in [13]. It achieves an extinction ratio greater than 3dB, limited by the amplitude differences of the symbols pertaining to IEEE 802.11ah 256-QAM constellation. However, authors seem to only evaluate the implementation of the WuTx based on software-defined radio. Direct access to IQ samples, as on a software-defined radio, is not supported by any off-the-shelf IEEE 802.11 device, thus, making this solution not valid for legacy IEEE 802.11 devices. The current IEEE 802.11ba specification also operates at the OFDM symbol level and uses OOK. However, by design, it is not compatible with legacy devices. Most recent IEEE 802.11ba draft contemplates two different signal modulations based on OOK: one achieving a rate of 250 kbps, and another one getting a slower rate of 62.5 kbps [17]. The faster 250 kbps modulation uses a Manchester code composed by two pulses 2 μ s duration per bit, and the slower 62.5 kbps modulation uses a Manchester code with repetition, using four pulses with 4 μ s duration, obtaining a bit duration of 16 μ s [18].

B. CHALLENGES OF OOK-BASED WuS GENERATION WITH IEEE 802.11 OFDM PHY

An OFDM transmitter is a flexible radio that can create complex waveforms from digital data. OFDM can be used, with the right inputs, to generate amplitude-based waveforms that can be decoded by low-power receivers [13]. With regard to IEEE 802.11, OFDM was introduced with IEEE 802.11 OFDM PHY, which firstly appeared with IEEE 802.11a specification, published in 1999 to operate at the 5 GHz ISM band. Afterward, in 2003, IEEE 802.11g was published, which extended OFDM PHY for operation at the 2.4 GHz ISM band. IEEE 802.11 OFDM PHY data rates were improved subsequently with IEEE 802.11n High-Throughput (HT) in 2009 and again with IEEE 802.11ac Very High Throughput (VHT) published in 2013.

However, IEEE 802.11 OFDM PHY is not able to generate good quality OOK signals. The main challenge for creating an OOK modulation using IEEE 802.11 OFDM PHY is achieving sufficient extinction ratios. The extinction ratio, in OOK, is the relation between the amplitude of the “0” symbol and the amplitude of the “1” symbol. A greater extinction ratio signifies that “0” symbols are further away in the constellation from the “1” symbols, reducing the probability of errors in symbol detection. There are two IEEE 802.11 OFDM PHY procedures that add power to the OFDM symbol regardless of the bits being transmitted. Those reduce the extinction ratio by increasing the amplitude of “0” OOK symbols. The first one consists in the integration of four high amplitude pilot tones to each OFDM symbol. The second one is inherent to the constellations used in Symbol Mapping. The set of

symbols used by IEEE 802.11 OFDM PHY to modulate its subcarriers does not include any symbol with zero amplitude [19]. Both of these procedures add amplitude to the “0” OOK symbols that can be generated with IEEE 802.11 OFDM PHY, thus reducing the achievable extinction ratio.

In IEEE 802.11ba, these problems are sidestepped by the use of a modified IEEE 802.11 OFDM PHY, which allows setting subcarrier values to 0. This feature enables the generation of “0” OOK symbols with constant 0 amplitude. Additionally, the DC subcarrier, deactivated in the original IEEE 802.11 OFDM PHY, is also enabled in IEEE 802.11ba to help with the generation of smoother pulses for “1” OOK symbols. The contributors to the IEEE 802.11ba have reached good results in synthesizing OOK symbols with this technique, called Multi-Carrier OOK (MC-OOK) [20], [21].

However, since the generation of OOK modulations with good extinction ratios is impossible using legacy IEEE 802.11 OFDM PHY, an alternative modulation needs to be devised. Such an alternative would enable the generation of an amplitude-based signal capable of bearing digital information using an unmodified IEEE 802.11 OFDM PHY transmitter.

Next section presents the structure of the earlier releases of IEEE 802.11 OFDM PHY, as well as a procedure to produce an amplitude-based signal with them.

IV. STRUCTURE OF IEEE 802.11A/G OFDM PHY AND AMPLITUDE-BASED SIGNAL GENERATION

IEEE 802.11a/g are the most widely supported IEEE 802.11 amendments compatible with IEEE 802.11 OFDM PHY and newer releases are backward compatible with them. For this reason, we have chosen 802.11a/g for the implementation of the WuR PoC presented in this paper. The extra features found in subsequent amendments do not impose modifications in relation to the WuR concept discussed and allow for the applicability of the same principles (see Section VII-A).

A. BLOCK STRUCTURE OF IEEE 802.11A/G OFDM PHY

This section presents the operating principles of IEEE 802.11a/g OFDM PHY, which, has been separated into several functional blocks. For each of the aforementioned blocks, a brief explanation of their operation is presented. The internal functioning of several of these blocks is relevant to the WuS generation procedure and is explained in more depth in Section V. The block structure of the IEEE 802.11a/g OFDM PHY is presented in Fig.2.

The entry bitstream is injected at the first IEEE 802.11a/g OFDM PHY block, the Scrambler, which adds a pseudo-random sequence, known by both receiver and transmitter, to the entry bitstream. Randomization of the entry bitstream decreases the probability of systematic errors, reduces the bias on reception and, finally, aids in reducing the average signal Peak to Average Power Ratio (PAPR). Afterward, the output of the Scrambler block is encoded on the Convolutional Coder block, using a coding rate between 1/2 and 3/4. Once coded, the resulting bitstream is separated into blocks

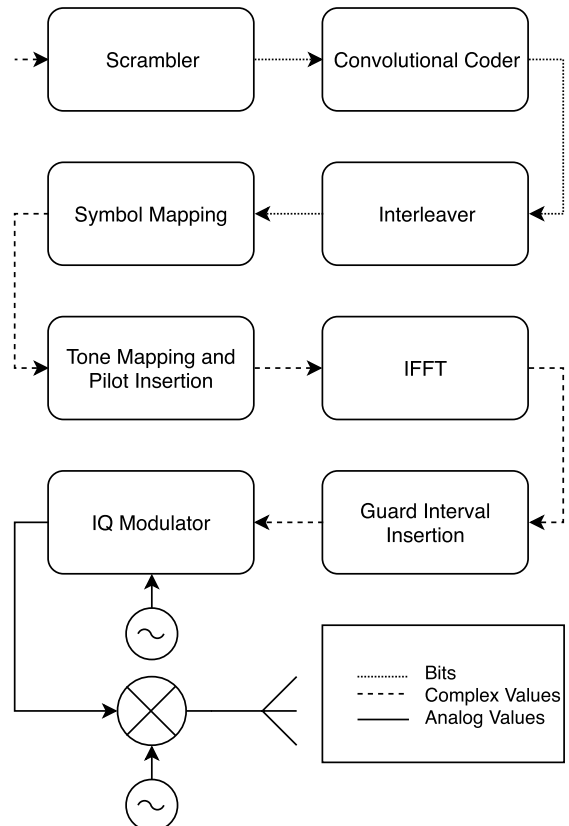


FIGURE 2. IEEE 802.11a/g OFDM PHY block structure for the data path. This block structure is also applicable to IEEE 802.11n/ac OFDM symbol generation. However, spatial multiplexing has to be taken into account.

of bits and their contents are interleaved by the Interleaver block. Interleaving reduces the likelihood of error bursts and improves the effectiveness of the convolutional code. Subsequent blocks, i.e., from Symbol Mapping to IQ Modulation, perform the transformation of the bit block into an OFDM symbol. First of all, the Symbol Mapping block converts the binary values from the bit block into complex symbols, using one of the four available constellations: BPSK, QPSK, 16-QAM or 64-QAM. Thus, the bit block output by the Interleaver results in a symbol block containing 48 complex samples. Then, four maximum amplitude symbols are added through the Tone Mapping and Pilot insertion block. Pilot tone addition increments the number of symbols in the block from 48 to 52. Each of the symbols contained in the symbol block, also named subcarrier or tone, represents one of the samples of the OFDM symbol in the frequency domain. Next, the 52 subcarriers are padded with “0” symbols, increasing the size of the symbol block to 64 samples. Later, the symbol block is sent to the Inverse Fast Fourier Transform (IFFT) block, which applies to it a 64 point IFFT. The output of the IFFT block is a sequence of 64 time-domain data samples, which are the values of the OFDM symbol in the time domain. Finally, the cyclic prefix is prepended to the 64 sample time domain symbol in the Guard Interval Insertion block. The cyclic prefix, which compromises the last 16 samples of the

time domain OFDM symbol, is added in order to mitigate the effect of multipath propagation on the OFDM symbol and keep inter-carrier interference low. Thus, the final OFDM symbol consists of a total of 80 time-domain samples, which are sent to the IQ Modulator block. The modulator transforms the samples of the OFDM symbol into the analog domain at a rate of 20 Msps. The final OFDM symbol is an analog waveform 4 μ s long. Subsequently, the generated OFDM symbol is sent through the RF front end.

B. POSSIBLE WAVEFORMS FOR WuS GENERATION

To study the available waveforms with IEEE 802.11 OFDM PHY, a simulation of the last stages of IEEE 802.11a/g OFDM PHY transmitter (i.e., from Symbol Mapping to Guard Interval Insertion) was developed. The MATLAB WLAN Toolbox did not provide explicit functional support to implement only these subset of stages from the complete IEEE 802.11a/g OFDM PHY pipeline. Therefore, the simulation framework for this task was implemented using MATLAB standard library functions. Nonetheless, the results obtained in this simulation framework were validated a posteriori with the output waveforms obtained with MATLAB WLAN Toolbox on equivalent inputs. This reduced simulation framework was only used for this task, while the rest of the methodological results presented in this paper are derived from the full IEEE 802.11 stack provided by MATLAB WLAN Toolbox.

Since OOK modulated signals were discarded due to the impossibility of generating “0” OOK symbols with close to null power (see Section III-B), other types of waveforms were considered. Using the simulation framework developed, the investigation focused on symbol blocks that produced OFDM symbols with pronounced peaks. The presence of one peak concentrates the symbol energy on a very narrow temporal interval, achieving a very high PAPR. Using this type of signaling, two possible symbols can be derived: one with a very high PAPR, henceforth referred to as *Peak Symbol* and another with a very low PAPR referred to as *Flat Symbol*. This Peak-Flat modulation deviates greatly from the usual OFDM symbols used in IEEE 802.11 OFDM PHY, which are constructed with mechanisms devised to limit their PAPR. This deviation can introduce problems related to clipping that can affect both the transmitter and the receiver. The former are discussed in more depth in Section VII-B. On the receiver side, the main possible impairment derived from clipping is an increase of difficulty on peak detection. Therefore, we propose two receiver alternatives for Peak-Flat modulation. The first receiver is based on a peak detector circuit that discriminates between the Peak and Flat Symbols based on the presence of significant peaks on the waveform. The other is a standard OOK receiver. Peak symbols, outside of the peak region, present a lower envelope compared to regular OFDM symbols, since most of their energy is concentrated at the peak. For this reason, the Peak-Flat modulation can be received as an OOK modulation with imperfect extinction ratio. This receiver is especially interesting as its performance

is unaffected by the clipping suffered by the Peak Symbols. Both receiver alternatives are presented in Section VIII.

Following, Sections V and VI introduce the methodology for the generation of such signals using data bits from higher layers on the IEEE 802.11 OFDM PHY, particularizing for the IEEE 802.11g transmitter used as PoC.

V. GENERATION OF THE PEAK SYMBOL

The discrete version of the Fourier Transform, the Discrete Fourier Transform (DFT) is instrumental in the generation of OFDM signals. The Inverse DFT (IDFT) transforms the symbol block derived from the bitstream into the OFDM symbol that is sent through the radio interface. DFT and its inverse share many properties with their analog counterpart, the Fourier Transform. One of them is frequency scaling, relating the temporal signal length with its transform signal length in the frequency domain, and vice versa. Signal expansion in the frequency domain leads to signal contraction in the time domain. The complete proof of this property for DFT can be found in [22].

The relationship between this property and PAPR is the following: generation of a wide constant pulse in the frequency domain leads to a very narrow waveform in the time domain, with very high PAPR, being most of its energy contained on a very narrow temporal region, i.e., a peak.

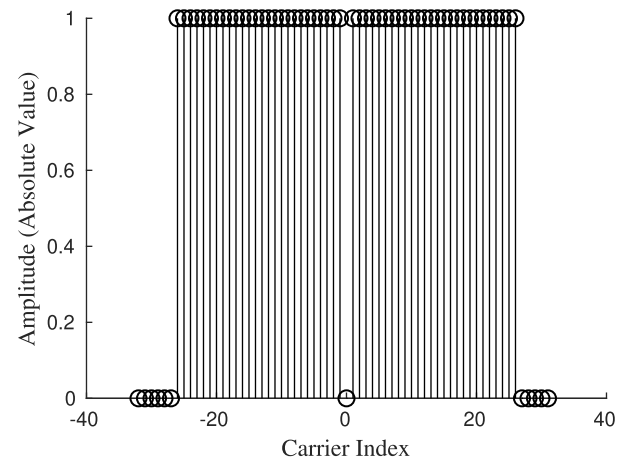


FIGURE 3. Amplitude of peak symbol subcarriers in frequency domain, defined in (1).

A. IDEAL PEAK SYMBOL

With the aforementioned relationship in mind, the conclusion is to use the widest possible constant waveform in the frequency domain, made up of samples of equal value. In IEEE 802.11 OFDM PHY, the closest implementation is a uniform symbol block. This block is created by assigning the same value to all the available OFDM subcarriers. Using IEEE 802.11a/g, the resulting symbol block is described mathematically in (1), where k represents the subcarrier index, and shown in Fig.3. This ideal result does not include the effects of pilot tone addition, these are addressed in Section III-B). IEEE 802.11g specifies that values for the

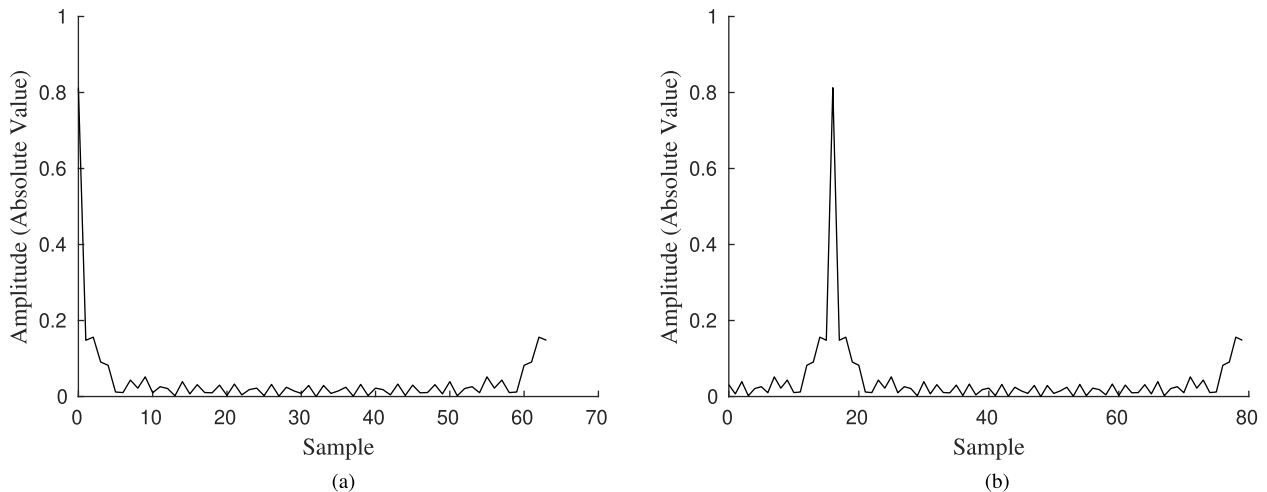


FIGURE 4. Amplitude of the ideal Peak Symbol in time domain described in (2). Note that after Guard Interval addition, the peak is delayed 16 samples. (a) Before Guard Interval insertion, 64 samples. (b) Amplitude of the OFDM symbol after Guard Interval insertion, 80 samples.

subcarrier with index 0 as well as the subcarriers that belong to the ranges going from -27 to -32 and from 26 to 31 must set to “0” [19].

$$X[k] = \begin{cases} 0 & k < -26 \\ 1 & -26 \leq k < 0 \\ 0 & k = 0 \\ 1 & 0 < k < 26 \\ 0 & k \geq 26 \end{cases} \quad (1)$$

The ideal OFDM symbol is the result of a 64 point IFFT to the 64 sample sequence generated by (1). In the time domain, the symbol adopts the expression of (2), where n corresponds to the sample index, which goes from 0 to 63. A plot based on (2) is shown in Fig.4a. The IEEE 802.11a/g OFDM PHY adds a guard interval of 16 samples to the OFDM symbol. The values of the OFDM symbol during this guard interval, or cyclic prefix, consist of a repetition of the last 16 samples of the OFDM symbol. The resulting OFDM symbol with guard interval is 80 samples long and is shown in Fig.4b. This OFDM symbol, which presents the highest PAPR attainable using IEEE 802.11a/g OFDM PHY, is the ideal Peak Symbol.

$$x[n] = \frac{1}{64} \frac{\sin(2\pi \frac{53}{64}n)}{\sin(2\pi \frac{1}{64}n)} - 1, \quad 0 \leq n \leq 63 \quad (2)$$

Ideally, the Peak Symbol can be produced by any uniform symbol block independently of the complex value used to initialize its 52 samples. All possible constellation symbol values supported by IEEE 802.11 OFDM PHY produce a waveform with the same shape and PAPR, although, with different scale factors.

The implementation of the Peak Symbol devised on this section using a complete IEEE 802.11a/g OFDM PHY presents an important challenge. The access to the symbol mapping stage, which produces the symbol block studied in this section, is not supported in any commercial IEEE 802.11

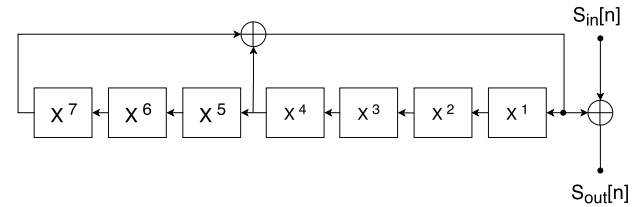


FIGURE 5. Scrambler used in IEEE 802.11 OFDM PHY [19].

transmitter implementation. For this reason, the uniform symbol block required for the generation of the Peak Symbol must be realized using the input bitstream at the beginning of the data path presented in Fig.2.

The following sections present the solutions taken in order to build the Peak Symbol from the bitstream at the entry of the IEEE 802.11g OFDM PHY data path.

B. ADDRESSING THE EFFECT OF THE SCRAMBLER BLOCK

The first block of the IEEE 802.11g OFDM PHY data path is the Scrambler. Its purpose is to randomize the input bitstream in order to avoid long runs of “0” or “1”. Randomization minimizes both the average PAPR of OFDM symbols and the DC bias at the reception. The IEEE 802.11 scrambler is implemented using a Linear Feedback Shift Register (LFSR) with the characteristic polynomial found in (3). The Scrambler is shown in Fig.5.

$$S[x] = 1 + x^4 + x^7 \quad (3)$$

The standard specification determines that the seed used to initialize the LFSR must change at the start of each frame transmission [19]. Most IEEE 802.11 OFDM PHY implementations do not provide read or write access to the scrambler seed. This makes the seed an unknown value. Nonetheless, in some cases, the scrambler seed can be determined using information external to the transceiver as pointed

out by [23]. Various transmitters use either a constant seed to initialize the LFSR, or one that can be predicted using data external to the IEEE 802.11 OFDM PHY, such as the MAC address of the transceiver and the number of transmitted bits.

In order to generate the Peak Symbol, a controlled bit sequence is required at the output of the Scrambler. Therefore, the randomization introduced by the scrambler must be compensated. If the initialization seed to be used by the Scrambler is known, then, the effect of the Scrambler can be canceled. This can be done by scrambling the input bitstream in advance, using the same bit sequence that the Scrambler will generate. The proof of this solution can be seen in (4)-(7). $x[n]$ consists of the intended bit sequence at the output of the scrambler, $y[n]$ the pseudo-random bit sequence generated by the Scrambler, $s_{in}[n]$ the sequence at the input of the Scrambler, and finally, $s_{out}[n]$ the output sequence of the Scrambler.

$$s_{in}[n] = y[n] \oplus x[n] \quad (4)$$

$$s_{out}[n] = s_{in}[n] \oplus y[n] \quad (5)$$

$$s_{out}[n] = x[n] \oplus y[n] \oplus y[n] \quad (6)$$

$$s_{out}[n] = x[n] \quad (7)$$

As a summary, the effects of the scrambler can be compensated only if the Scrambler initialization seed is known in advance and the input sequence is pre-scrambled.

TABLE 1. Parameters of the convolutional coder used in IEEE 802.11 OFDM PHY.

Symbol	Value
r	2
k	7
g_0	1338
g_1	1718

C. ADDRESSING THE EFFECT OF THE CONVOLUTIONAL CODER BLOCK

The Convolutional Coder block encodes the data with a Forward Error Correcting (FEC) code. The convolutional coder used presents the common parameters, where r represents the coding rate, k is the window length, and g_0 and g_1 are the generator polynomials, all defined in Table 1. The coder, shown in Fig.6, generates two output bits for every input bit and has a memory of 6 bits. The coding rate is by default 1/2, additional coding rates of 2/3 and 3/4 are obtained from the same convolutional coder structure by using Puncturing, which removes bits from the output of the coder. These bits are introduced again in the receiver, before the decoder block, as “0” values. This technique reduces the redundancy at the expense of reducing the capability to recover from errors. The use of the convolutional coder is required at all data rates supported on IEEE 802.11a/g. On the following releases, the presence of a convolutional coder on the device is still a requirement. In this way, the solution presented here is compatible with IEEE 802.11n/ac.

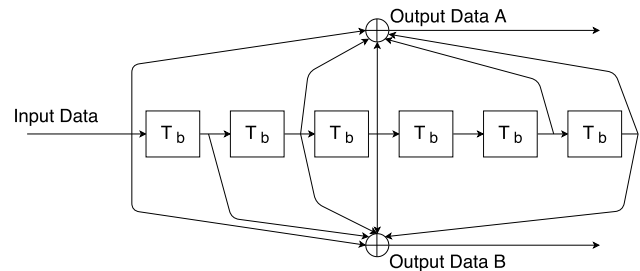


FIGURE 6. Convolutional Coder used in IEEE 802.11 PHY. Note that for each bit input, two outputs, Data A and Data B are generated. Each T_b block represents one bit delay [19].

For the purpose of having a certain sequence of bits at the input of the symbol mapping stage, the Convolutional Coder is the most challenging block to work with. Not every bit sequence is possible at the output, due to the effect of coding and the redundancies added. However, there are two input bit sequences that are not modified by the addition of coding and, hence, are equal at the output, only multiplied in size by the inverse of the coding rate used.

The first bit sequence is a uniform input sequence of “0” bits, which results on another uniform output sequence of “0” bits, but grown in size, i.e., a sequence of 50 “0” at the input, coded with a rate of 1/2, results in a sequence of 100 “0” at the output. As seen in (8)-(11), for each “0” at the input, two “0” are obtained at the output.

$$s[n] = \{0, 0, 0, 0, 0, 0\} \quad (8)$$

$$x = 0 \quad (9)$$

$$y_a = x \oplus s[2] \oplus s[3] \oplus s[5] \oplus s[6]$$

$$= 0 \oplus 0 \oplus 0 \oplus 0 \oplus 0 = 0 \quad (10)$$

$$y_b = x \oplus s[1] \oplus s[2] \oplus s[3] \oplus s[6]$$

$$= 0 \oplus 0 \oplus 0 \oplus 0 \oplus 0 = 0 \quad (11)$$

where x represents the input bit, $s[n]$, the 6-bit wide scrambler state, y_a the Data A output of the coder, obtained by applying g_0 to x , and, finally, y_b the Data B output, generated in a similar way by g_1 . Both Data A and Data B correspond to the outputs displayed in Fig.6.

Another interesting input sequence consists in the binary inverse of the former, i.e., all bits set to “1”. If the coder state bits are also set all to “1”, the output for this sequence is a uniform “1” sequence, with its length multiplied by the inverse of the coding rate. The number of XOR operations in both branches of the coder is five, which is an odd number. Having an odd number of XOR operation with “1” logic values at the inputs always result in “1”. This can be seen in (12)-(15), using the same variable notation that was used in (8)-(11).

$$s[n] = \{1, 1, 1, 1, 1, 1\} \quad (12)$$

$$x = 0 \quad (13)$$

$$\begin{aligned}
 y_a &= x \oplus s[2] \oplus s[3] \oplus s[5] \oplus s[6] \\
 &= 1 \oplus 1 \oplus 1 \oplus 1 \oplus 1 \\
 &= (((1 \oplus 1) \oplus 1) \oplus 1) \oplus 1 \\
 &= (((0 \oplus 1) \oplus 1) \oplus 1) \\
 &= ((1 \oplus 1) \oplus 1) \\
 &= (0 \oplus 1) = 1
 \end{aligned} \tag{14}$$

$$\begin{aligned}
 y_b &= x \oplus s[1] \oplus s[2] \oplus s[3] \oplus s[6] \\
 &= 1 \oplus 1 \oplus 1 \oplus 1 \oplus 1
 \end{aligned} \tag{15}$$

Note that the result in (15) is only applicable when the generator polynomials have an odd number of non-zero terms, a condition that is always met in IEEE 802.11a/g/n/ac. Those specifications use the odd-numbered generator polynomials shown here. Moreover, the Convolutional Coder introduces transitorial effects that affect the generation of different symbols. This last issue is addressed in Section VI-A.

In conclusion, two uniform binary sequences can cross the coder unmodified, i.e., all “1” and all “0” sequences. Next section, the following block on the IEEE 802.11 OFDM PHY will be presented, the Interleaver.

D. ADDRESSING THE EFFECT OF THE INTERLEAVER BLOCK

The purpose of the Interleaver is to distribute bit errors uniformly, in order to maximize FEC coding effectiveness. First of all, it separates the incoming bitstream on blocks of an integer number of bits, which will be jointly encoded in the same OFDM symbol on later stages. The number of bits per block depends on the modulation used on the Symbol Mapping block. The Interleaver operates in the generated bit block with two steps. The first step distributes the adjacent bits within the block so that they will be encoded into non-adjacent subcarriers. This step protects the bit block against error bursts caused by narrow-band fading. The second step is only applied when high data rates are employed, which use QAM modulations. On those situations, the bits assigned to each subcarrier are distributed among the less and more significant bits of the QAM constellation symbol. This mechanism compensates for the greater systematic error rate that the least significant bits of QAM symbols suffer.

The effect of the Interleaver block can be avoided by pre-interleaving the sequence at the data input, so that bits will fall in their intended positions after the interleaving process. However, this complicates further the task of finding the correct input to generate an arbitrary bit sequence as the pre-interleaved one needs to be a code word of the convolutional code. To avoid this pitfall, the two uniform “0” and “1” sequences can also be used. As they are uniform sequences, they cannot be modified by interleaving. Changing the positions of the elements of a uniform sequence does not change the resulting sequences.

E. EFFECT OF THE SYMBOL MAPPING BLOCK

After the previous blocks, which operate with binary values, the Symbol Mapping block is found. Symbol Mapping converts the bit blocks at the output of the Interleaver into symbol blocks. Each symbol block contains 48 complex symbol values in IEEE 802.11a/g [19]. These symbols are also referred to as subcarriers or tones. Subsequent amendments can support a higher number of subcarriers per OFDM symbol, with up to 108 symbols in IEEE 802.11n [24] and up to 468 in IEEE 802.11ac [25]. The conversion from bits into symbols is performed with one of the available constellations in IEEE 802.11 OFDM PHY: BPSK, QPSK, 16-QAM, 64-QAM, and 256-QAM. The first four constellations are supported in IEEE 802.11a/g/n and the last one, 256-QAM, is only supported in IEEE 802.11ac.

Using the results from previous Sections V-B, V-C and V-D we have found two interesting binary sequences that, at the output of the Interleaver, form uniform bit blocks. These bit blocks, when coded by the Symbol Mapper, are able to generate uniform symbol blocks. As proven in Section V-A, coding a uniform symbol block into an OFDM symbol generates the Peak Symbol waveform. However, not all symbols supported by the IEEE 802.11 constellations can be generated from these inputs. Due to the uniformity of the bit blocks used, only symbols that encode a series of “0” or “1” bits can be generated. For the IEEE 802.11g specification, which is used for the PoC, the remaining available symbol values for Peak Symbol generation are found in Table 2.

TABLE 2. Possible symbol values derived from uniform bit blocks.

Modulation	Symbol value	Coded Bits
BPSK	-1	“0”
BPSK	+1	“1”
QPSK	+1 + 1j	“11”
QPSK	-1 - 1j	“00”
16-QAM	1 + 1j	“1111”
16-QAM	-3 - 3j	“0000”
64-QAM	3 + 3j	“111111”
64-QAM	-7 - 7j	“000000”

Next section presents the Pilot Tone Insertion and Tone Mapping block and the effects of pilot tone addition to the Peak Symbols.

F. EFFECT OF PILOT TONE ADDITION

After symbol mapping, pilot tone addition follows. The analysis of this block will be focused on the IEEE 802.11a/g specification. Pilot tones are inserted at the Tone Mapping and Pilot Tone Insertion block, which adds 4 pilot symbols to the existing symbol block, increasing its length from 48 to 52. Pilot tones act as reference values for the receiver. The pilot tones are added on the following sub-carrier indexes: 7, 21, -7, and -21. The amplitude of pilot tones is fixed at 1. Three of the tones share the same phase, and only one, with the index 21, shows an opposite phase.

The pilot tone contribution to the symbol block is shown on sequence $P_{-26,26}$ from (16).

$$\begin{aligned} P_{-26,25} = \{ &0, 0, 0, 0, 0, 1, 0, 0, 0, 0, 0, 0, \\ &0, 0, 0, 0, 0, 1, 0, 0, 0, 0, 0, 0, \\ &0, 0, 0, 0, 0, 0, 1, 0, 0, 0, 0, 0, \\ &0, 0, 0, 0, 0, 0, 0, -1, 0, 0, 0, 0, 0 \} \quad (16) \end{aligned}$$

The phase of the pilot tones is changed after each OFDM symbol. The values of the pilot tones are multiplied by -1 or $+1$ following a pseudo-random sequence. This sequence is equal to the one generated by the Scrambler (see Section V-B) but, substituting “0” by “ -1 ” and “1” by “ $+1$ ” [19]. Due to this dynamic phase component, there are two pilot tone combinations that alternate: the first, with mostly positive phase, formed by three “ $+1$ ” and one “ -1 ”; and the second, with mostly negative phase, formed by three “ -1 ” and one “ $+1$ ”.

The presence of these pilot tones changes the content of the symbol block, breaking its uniformity and altering the resulting OFDM symbol. In this way, the obtained PAPR of the ideal Peak Symbol is degraded after pilot tone addition. The magnitude of this effect on the PAPR depends on the value of the subcarriers conforming the symbol block. e.g., if the value of the majority of the pilot tones is “ -1 ”, the PAPR of the resulting Peak Symbol will be higher if the rest of its subcarriers are also “ -1 ”, and lower if they are “ $+1$ ”. The simulator described in Section IV-B was used to generate Peak Symbols with all the remaining subcarrier values (see Table 2) and pilot tone combinations. The result of this study can be found in Table 3.

TABLE 3. PAPR obtained for each symbol and pilot tone phase combination.

Modulation	Symbol value	Negative pilot tones PAPR(dB)	Positive pilot tones PAPR(dB)	Average PAPR(dB)
BPSK	-1	17.39	16.59	16.99
BPSK	+1	16.59	17.39	16.99
QPSK	$1 + 1j$	16.76	17.24	17.00
QPSK	$-1 - 1j$	17.24	16.76	17.00
16-QAM	$1 + 1j$	15.17	16.27	15.72
16-QAM	$-3 - 3j$	17.35	16.99	17.17
64-QAM	$3 + 3j$	16.16	16.90	16.53
64-QAM	$-7 - 7j$	17.38	17.05	17.22

The optimal non-ideal Peak Symbol should present the highest average PAPR. In this way, a higher PAPR indicates greater similarity to the ideal peak waveform presented in Section V-A. The average PAPR is derived by averaging the PAPR of the two Peak Symbols generated by a given subcarrier value, one with each pilot tone combination (in-phase and on opposite phase). Accordingly, the best subcarrier value, with an average PAPR of 17.22 dB, is 64-QAM “ $-7 - 7j$ ”, which encodes 6 “0” bits. The BPSK “ -1 ” and “ $+1$ ” values, representing “0” and “1” logic values, are also interesting. They present best PAPR results when the pilot tones are in phase, with a PAPR of 17.39 dB. In contrast, Peak Symbols built using BPSK subcarrier values do not perform

as well when the pilot tones are on the opposite phase. The average PAPR for both BPSK “ $+1$ ” and “ -1 ” is 16.99, approximately 0.2 dB lower than the average PAPR obtained by 64-QAM “ $-7 - 7j$ ”.

G. BIT SEQUENCES USED TO GENERATE THE PEAK SYMBOL

Previous Sections V-B, V-C, V-D and V-E propose several bit sequences that can go through the blocks of the IEEE 802.11 OFDM PHY data path and produce uniform symbol blocks. These blocks are capable of generating Peak Symbols (see Section V-A) at the output of the IEEE 802.11 transmitter. Using these results, the conditions that an entry bit sequence capable of generating a Peak Symbol must fulfill can be obtained.

These are summarized in the following statements:

- 1) The bit sequence must be pre-scrambled in order to avoid the randomization introduced by the scrambler block.
- 2) The bit sequence at the output of the scrambler must be uniform, i.e., either all “0” or all “1”. This way, modifications introduced by coding and interleaving are avoided.
- 3) The length of the sequence must be equal to the OFDM symbol payload length so that the sequence is long enough to modulate all the subcarriers with the same symbol value.
- 4) The sequence must be aligned with OFDM symbol boundaries. The entire bit sequence must be encoded jointly in the same OFDM symbol. If the sequence is divided into two OFDM symbols, uniformity will be lost.

We now present the binary sequences that can generate the Peak Symbols based on subcarrier values BPSK “ -1 ” and 64-QAM “ $-7 - 7j$ ”, highlighted in Section V-F. Nonetheless, the Peak Symbols featuring the remainder of symbol values presented in Section V-E can be generated using the same principles.

- For BPSK “ -1 ” with a coding rate of 1/2:
This configuration corresponds to the 6 Mbps data rate used by IEEE 802.11a/g. To generate the Peak Symbol, a uniform sequence of 24 “0” bits is used. The input sequence must be pre-scrambled before being sent to the IEEE 802.11 OFDM PHY data path. This sequence generates a uniform symbol block with all subcarriers modulated to “ -1 ”. The OFDM symbol generated by this symbol block presents the waveform shown in Fig. 7a.
- For 64-QAM “ $-7 - 7j$ ” with a coding rate of 3/4:
This configuration corresponds to the 54 Mbps data rate used by IEEE 802.11a/g. To generate the Peak Symbol, a uniform sequence of 216 “0” bits is used. The sequence must be pre-scrambled before being sent to the IEEE 802.11 OFDM PHY data path. This sequence generates a uniform symbol block with all subcarriers modulated to “ $-7 - 7j$ ”. The OFDM symbol generated

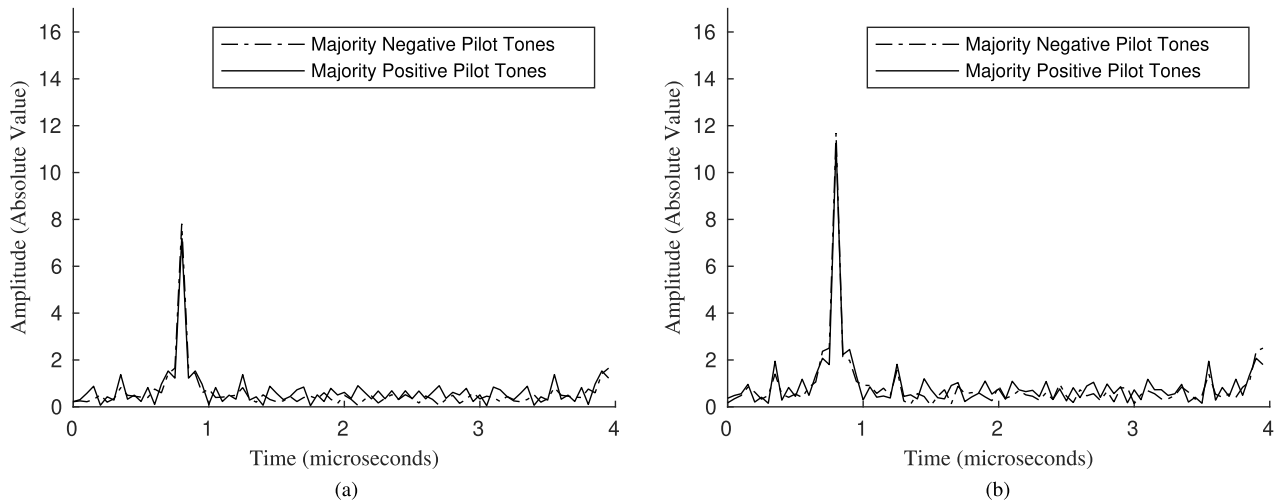


FIGURE 7. Amplitude of best case non-ideal peak symbols. (a) Amplitude of the peak symbol using BPSK symbol -1 . (b) Amplitude of the peak symbol using 64-QAM symbol $-7 -7j$.

by this symbol block presents the waveform shown in Fig.7b.

VI. GENERATION OF THE FLAT SYMBOL

To complement the Peak Symbol, a Flat Symbol, with the minimum possible PAPR has to be designed. This section presents the procedure used to generate the Flat Symbol and proposes one example of Flat Symbol generation.

A. PROCEDURE TO OBTAIN THE FLAT SYMBOL

The Flat Symbol is the OFDM symbol that presents the minimum PAPR for a given modulation and coding rate combination. As a consequence, the Flat Symbol must be constructed using the same modulation and coding scheme as its complementary Peak Symbol. The reason for this requirement is that IEEE 802.11g/a OFDM PHY frames combining two different modulation schemes after the SIGNAL field are not supported [19]. Consequently, there is a Flat Symbol for each of the Peak Symbols presented in Section V-E. Similar to the peak Symbol, the Flat Symbol is built using the input bitstream to the IEEE 802.11 OFDM PHY. Then, in order to generate the Flat Symbol, the bit sequence constructing the OFDM symbol with minimum PAPR must be found. Nevertheless, the bit sequence that produces the Flat Symbol has to fulfill one condition: it cannot introduce any inter-symbol interference. Such interference is produced by the six sample memory of the convolutional coder. Depending on its contents, the coder could modify the first six values at the start of the following bit block, thus, introducing unintended values into the bit block and altering its resulting OFDM symbol. In order to avoid interference, the state of the convolutional coder has to be reset at the end of each bit block. For this purpose, the last six bits of the entry bit sequence have to be either “0” or “1”. The value of these last bits needs to be equal to the value used to generate the corresponding Peak Symbol. e.g., if the corresponding Peak

Symbol is generated by a block of “0” bits, then, the last six bits of its matching Flat Symbol have to be “0” as well. In this way, the search space for the optimal Flat Symbol encompasses all bit sequences long enough to form an OFDM symbol that ends with either six “1” or six “0”.

B. EXAMPLE OF FLAT SYMBOL GENERATION

With this criterion, we propose finding the bit sequence that generates the Flat Symbol for one of the Peak Symbol examples proposed in Section V-G: BPSK “ -1 ” with $1/2$ coding rate. The bit block length for this modulation and coding rate is of 24 bits. Consequently, the search space for the optimization problem becomes all sequences of 24 bits that end with 6 consecutive “0” bits, with a total of 2^{18} possible sequences. This is still a tractable number of sequences to be explored exhaustively. In this way, the PAPR of the OFDM symbols generated by every possible bit sequence is calculated. The resulting Flat Symbol for “BPSK” “ -1 ” with coding rate $1/2$, generated by the bit sequence $s[n]$ from (17), presents an average PAPR of 3.09 dB. The resulting Peak Symbol waveform is shown in Fig.8.

$$s[n] = \{1, 1, 0, 0, 1, 1, 1, 0, 1, 0, 1, 1, 0, 1, 0, 1, 0, 0, 0, 0, 0, 0, 0, 0\} \quad (17)$$

VII. SIMULATION OF THE WAKE-UP TRANSMITTER

Once the bit sequences that generate both the Peak and Flat Symbols for a given modulation were found, a PoC of the WuTx is proposed. The WuTx is based on IEEE 802.11g and is implemented using the MATLAB WLAN Toolbox simulation tool. The MATLAB WLAN toolbox implementation allows to set the initial state of the scrambler, so the prerequisite detailed in Section V-B to use the Peak-Flat modulation is met. The PoC is particularized for the following parameters: the modulation used is BPSK, the symbol value used on Peak Symbols is “ -1 ”, and the coding rate used is $1/2$. On this

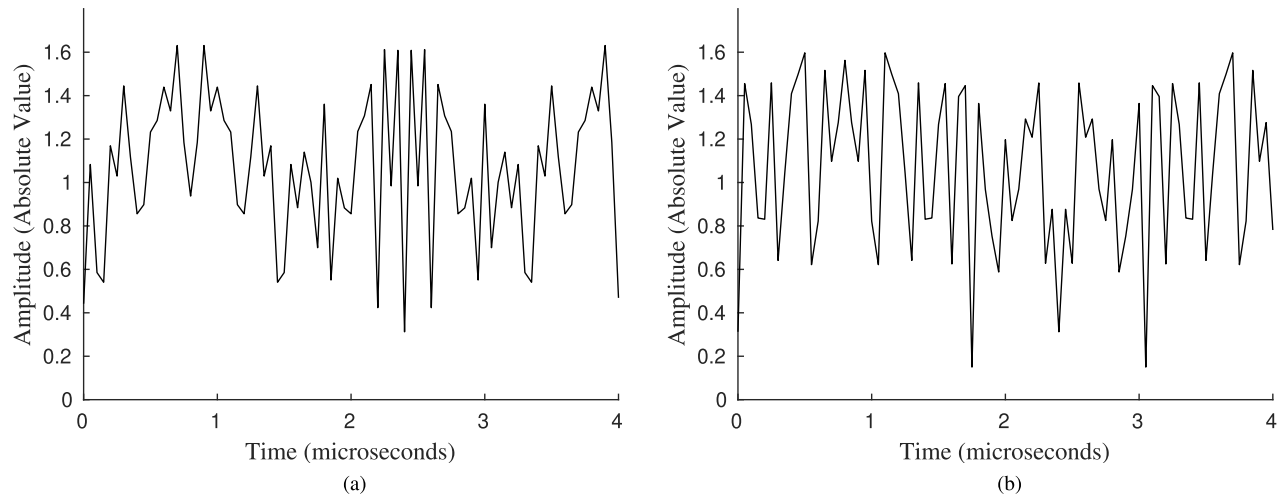


FIGURE 8. Amplitude of the flat symbol generated by the binary sequence presented in (17). Note that its maximum amplitude is significantly lower than the peak of its respective peak symbol presented in Fig.7a. (a) Amplitude of the flat symbol using pilot tones with mostly positive phase. (b) Amplitude of the flat symbol using pilot tones with mostly negative phase.

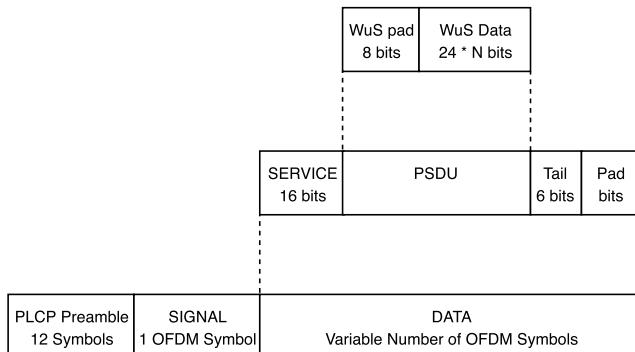


FIGURE 9. IEEE 802.11 frame structure of the proposed WuS for the specific case of BPSK and coding rate 1/2.

PoC the Peak Symbol is used to encode the “0” logic value and the Flat Symbol is used to encode the “1” logic value. This would be the most advisable codification if the receiver was based on OOK detection. For such a receiver, the Peak Symbol produces a low level at sampling time, whereas the Flat Symbol produces a high level. On this PoC of the WuTx, the bitstream that generates the WuS is injected at PSDU level following the legacy non-HT IEEE 802.11 frame structure [19], represented in Fig.9. Only the PSDU field of the IEEE 802.11 frame is modified by the WuS. The remaining fields of a standard IEEE 802.11 frame are not altered by this implementation.

Following steps describe the method for WuS generation using the Peak-Flat modulation (see Sections V and VI) with the WuTx proposed in this PoC. This method is compatible with any standard compliant IEEE 802.11a/g OFDM PHY transmitter, as long as the initial scrambler state is known.

- 1) Align the WuS bits to OFDM symbol length with padding. The first 16 bits corresponding to the IEEE 802.11 non-HT PPDU are occupied by the Service field, which is not part of the PSDU. Padding is

required to begin the WuS at the OFDM symbol boundary. In this way, 8 bits of padding are appended at the start of the PSDU. The padding completes the first OFDM symbol and allows the WuS to start on the second OFDM symbol of the PSDU. The alignment of the bitstream to OFDM symbols is required to generate the Peak-Flat modulation symbols (see Section V-G). After this step, the WuTx is ready to encode the WuS.

- 2) Append the WuS data. Add a bit block for each WuS payload bit. If the WuS bit value is “1”, append the 24-bit Flat Symbol sequence derived in Section VI-B. In the case of a “0” value, use the 24 bit “0” sequence for a Peak Symbol derived in Section V.
- 3) Pre-scramble the WuS to ensure the proper output sequence after the scrambler. After 2), the real Scrambler would have already scrambled the 24 bits pertaining to the first OFDM symbol of the PSDU. Therefore, the predicted scrambler state has to be advanced 24 bits, in order to align it with the real scrambler state. Subsequently, for every PSDU bit generated in step 2), advance the predicted scrambler state one bit and XOR the predicted scrambler result to that bit.
- 4) Transmit the resulting binary sequence, composed by the PSDU. The final PSDU includes the padding bits required to skip the first OFDM symbol as well as the pre-scrambled WuS bits, coded on one OFDM symbol each. The PSDU is now sent to the lower layers of the stack for transmission.

Consider the waveform generated by the WuTx and represented in Fig.10. The WuS displayed carries the WuS payload “010101010101010”. This sequence, which alternates Peak and Flat Symbols, displays the differences between the two possible waveforms of the Peak-Flat modulation. Peak Symbols, labeled as “0” feature their characteristic peak and the low amplitude region that follows it. In contrast, Flat Symbols, labeled as “1”, have less extreme values and a more

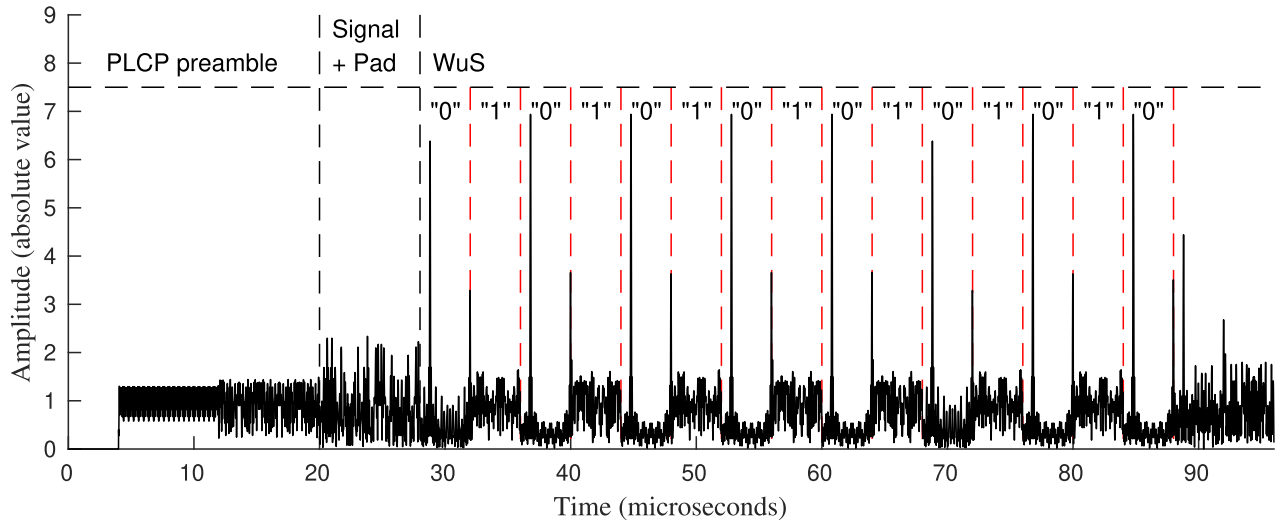


FIGURE 10. The actual generated WuS, encoding the binary value “01010101010101010” with peak symbols representing a logic “0” and flat symbols a logic “1”.

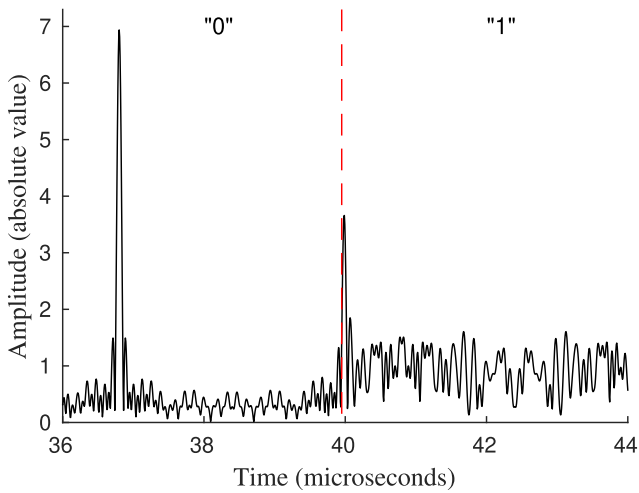


FIGURE 11. Detail of two symbols from the waveform displayed in Fig.10.

rectangular shape. As it can be better observed in Fig.11, the Flat Symbols that follow a Peak Symbol display a secondary peak with roughly half of the amplitude of the peak featured in the previous Peak symbol. This is caused by the MATLAB WLAN Toolbox implementation of windowing, occurring at the start of every OFDM symbol. The purpose of this mechanism, which in no way is fulfilled in this particular case, is to smooth OFDM symbol transitions.

A. APPLICABILITY TO OTHER IEEE 802.11N/AC OFDM AMMENDMENTS

IEEE 802.11n/ac OFDM PHY defines transmission modes entailing a signal processing chain that is compatible with the presented method. In this way, the described procedure can be applied to single spatial stream transmissions, i.e., from MCS 0 to MCS 7. This is valid as long as the transmitter is

configured to use the compulsory Convolutional Coder-based FEC and the optional space-time block coding feature is not in use.

B. PHY DERIVED IMPAIRMENTS

Non-idealities in the physical components of the transmitter, i.e., power amplifier non-linearity and saturation, can affect the regulatory compliance of Peak- Flat modulation. Even if Peak-Flat defines what is a completely valid IEEE 802.11 signal, the high dynamic range of Peak Symbols can introduce distortion and, as a consequence, out-of-band emissions.

To consider this possible issue, the compliance of Peak-Flat signals has been evaluated with a simulated non-ideal power amplifier. The simulations have been performed with MATLAB WLAN Toolbox spectrum compliance tools to check for out-of-band emissions against the spectral mask defined by IEEE 802.11a. To simulate a non-linear amplifier we have used a Rapp model with parameter $p = 3$. Additionally, we have also considered the Peak-Flat configuration that generates the highest PAPR (IEEE 802.11g with BPSK, with a maximum of 17.39 dB PAPR). The saturation power is expressed in dBm while considering a signal with mean average transmission power of 0 dBm. For example, the considered variant of Peak-Flat will have an average power of 0 dBm while having a peak power of 17.39 dBm.

As can be seen in Fig. 12, for a saturation A_{sat} value of 27 dBm, which causes no clipping, the signal remains completely inside the spectral mask.

In fact, Peak Flat can operate with an amount of distortion, even with saturation points below its peak power, while maintaining compliance. With an A_{sat} of 14.75 dBm, displayed in Fig. 13, the peak amplitude while clipped, maintains its compliance with the spectrum mask. For an A_{sat} lower than 14.75 dBm, Peak-Flat at 0 dBm transmitted power fails compliance tests. With lower A_{sat} values, compliance with

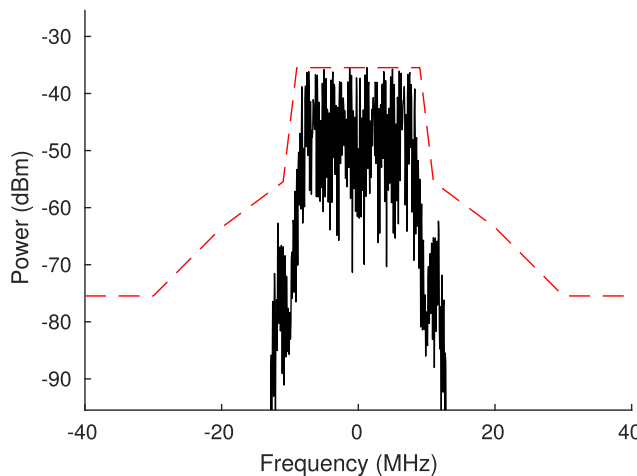


FIGURE 12. Spectrum of a peak signal with $A_{sat} = 27$ dBm. Dashed red line represents the spectral mask.

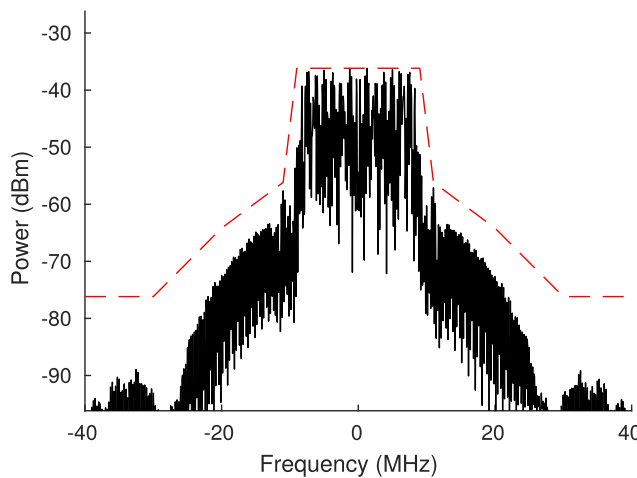


FIGURE 13. Spectrum of a peak signal with $A_{sat} = 14.75$ dBm. Dashed red line represents the spectral mask.

the spectrum mask is still possible, although, the transmitted power must be reduced. For example, if the mean average transmission power is reduced to -3 dB, the system remains compliant down to an A_{sat} of 11.75 dB.

In conclusion, Peak-Flat remains compliant with the IEEE 802.11a defined spectrum masks as long as the saturation power of the amplifier remains at most 2.64 dB

lower than the peak transmitted power, that must be adjusted accordingly. As with the rest of IEEE 802.11 signals, the final limit to allowed transmission power for Peak-Flat will depend on both the regional regulatory limits and the saturation limit imposed by the power amplifier of the device.

In the next section, two receiver architectures for the chosen Peak-Flat modulation will be presented.

VIII. WAKE-UP RECEIVER PROPOSALS

This section presents two architectural proposals for the WuRx, as well as a benchmark of their performance by means of simulations. This benchmark is performed on both receiver prototypes using Simulink. Both proposals consist of minimal designs using off-the-shelf components, and are not intended to be compared against the current WuRx state of the art, nor serve as optimal receivers for the Peak-Flat modulation. Thus, the receivers presented are conceived as a way to evaluate Peak-Flat modulation feasibility and to compare it with other modulations under the same conditions.

A. GENERAL ARCHITECTURE FOR THE WuRx

The proposed WuRx, shown in Fig.14, is composed of a Radio Front End and a Bit Decoder, which is an element that decodes the incoming analog waveform into a binary stream. The proposed Radio Front End consists of the following elements: an antenna, a band-pass filter (tuned to the 2.4 GHz ISM band), a Low Noise Amplifier (LNA), a band-pass filter and, finally, an envelope detector. Two different implementations are proposed for the Bit Decoder, the first is targeted at OOK signal decoding, the second is based on a peak detector. Next sections present both architecture proposals.

B. BIT DECODING USING AN OOK DETECTOR

The first WuRx Bit Decoder implementation follows the basic design for OOK signal detection. The working principle of this design applied to the Peak-Flat modulation is the following. The envelope for Flat Symbols is higher than the envelope for Peak Symbols, outside the peak region, as shown in Section V and as can be observed in Fig.10. Therefore, the amplitudes created by Peak and Flat Symbols are distinguishable. This receiver is additionally capable of decoding OOK-based modulations, like the one used in the current IEEE 802.11ba proposal.

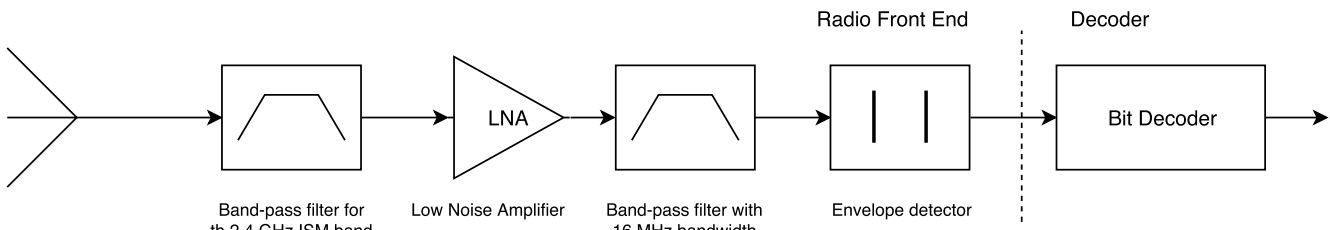


FIGURE 14. Structure of the proposed WuRx.

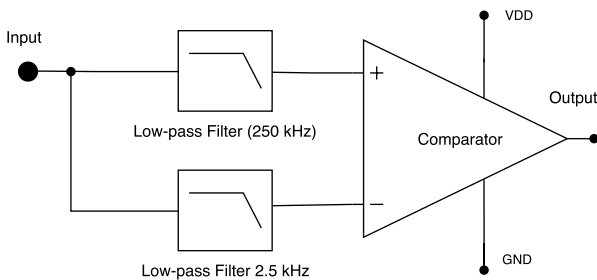


FIGURE 15. Structure of the proposed Bit Decoder based on OOK reception.

The proposed Bit Decoder follows a minimal implementation, two filters, and a comparator. A block diagram of the proposed design is shown in Fig.15. The first filter is tuned close to 250 kHz, matching it with the IEEE 802.11g OFDM symbol rate. The purpose of this filter is to smooth the envelope of the signal, in order to allow for the reliable detection of the amplitude level. The filter cutoff frequency is sufficient to smooth the contents of the OFDM symbol while providing a response fast enough to separate consecutive OFDM symbols. The second filter is tuned to a frequency that allows it to obtain an almost constant envelope from a regular IEEE 802.11 frame, i.e., from 2.5 kHz to 5 kHz. This range of frequencies was obtained heuristically on the simulations. The output of the second filter is used as the reference value for detection. Finally, a comparator is used to compare the output of both filters. If the output of the first filter (which tracks signal envelope) is higher than the one from the second filter (which provides the reference value), the comparator output becomes high. On the contrary, if the output from the first filter is lower than the reference value, the comparator output becomes low.

This architecture has been implemented using a Simulink model for evaluation. Both filters are implemented with a first-order RC filter, the first at 250 kHz, and, the second, at 2.5 kHz.

On this receiver architecture, in addition to the Peak-Flat modulation proposed in this paper, two other state-of-the-art WuR modulations were tested: the first is a 250 kBd OOK modulation with perfect extinction ratios, and the second, the current proposal for IEEE 802.11ba fast data rate. However, the receiver must be modified slightly in order to receive IEEE 802.11ba fast data rate. Since IEEE 802.11ba operates using $2\ \mu\text{s}$ OOK symbols, the bandwidth of the first low-pass filter is increased to a value close to 500 kHz.

In the following section, the proposed architecture using a peak detector will be presented.

C. BIT DECODING USING A PEAK DETECTOR

The second proposed implementation for the WuRx Bit Decoder distinguishes between both symbols by the presence of a peak. The working principle of this proposal is that, due to their own design, Peak Symbols produce a detectable peak,

well above from the maximum signal level produced by Flat Symbols. The presence of this peak can effectively be detected using a peak detector circuit.

The implementation of the Bit Decoder is composed of a peak detector circuit, a voltage divider, a low-pass filter, and a comparator. A block diagram of the proposed design is shown in Fig.16.

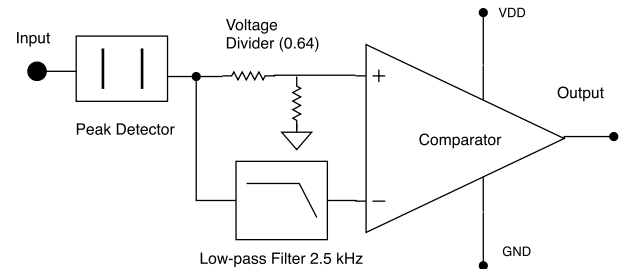


FIGURE 16. Structure of the proposed Bit Decoder based on a peak detection.

The peak detector is implemented using a Schottky diode, followed by a parallel capacitor for charge storage. When the input signal is greater than the diode voltage threshold, the capacitor will charge faster than when it is under the threshold, generating an asymmetry. When a peak is received, the peak detector charges fast, and then, after the peak ends, it discharges at a slower speed. This non-linear effect helps to increase the duration of the peak, which is originally 50ns (a single sample at 20 Msps). This increase in the duration of the peak protects the signal against the typical synchronization issues of feature limited electronics. To reduce the probability of false peak detection, a voltage divider is connected at the output of the peak detector. Without this component, whenever the peak detector output raised slightly above the average amplitude of the frame, a peak would be detected. The low-pass filter element in this receiver has the same purpose as the second filter of the OOK detector architecture, i.e., to provide a reference value based on the frame envelope. It is placed after envelope detection since this non-linear procedure changes the average amplitude of the received signal. Finally, the decoding decision is determined by the comparator output. The voltage divider output is connected to the comparator non-inverting input, whereas the low-pass filter output is connected to its inverting input. Using this configuration, a peak only produces a high level at the comparator's output when its amplitude, diminished by the voltage divider, is higher than the average envelope, provided by the low-pass filter. Conversely to the OOK receiver, the peak detector generates a high logic value for Peak Symbols and a low one for Flat Symbols.

For the Simulink implementation of this receiver, the filter keeping the frame reference level is, as well as for the OOK implementation, a first-order RC filter tuned at 2.5 kHz. The value for the capacitance used for the peak detector is 1nF and was heuristically determined using a parametric sweep

on the Simulink model. The Peak detector, jointly with the resistances of the voltage divider, increments the duration of the peak to $1\ \mu\text{s}$. The voltage divider uses resistances of $4\ \text{k}\Omega$ and $7.6\ \text{k}\Omega$. These values produce a divider with a rate close to 1.5, also heuristically obtained. The aggregate value of both resistances allows peaks to stay above the detection threshold for roughly $1\ \mu\text{s}$.

D. DECODER EVALUATION

To evaluate the proposed modulation, BER vs. SNR was simulated on an AWGN channel. Additionally, PER vs SNR was also simulated on TGn Channel B. All the simulations are performed for both of the considered WuRx architectures using different modulations. The noise type considered and the resulting SNR is specified at 20 MHz bandwidth. The equivalent noise bandwidth that affects the WuRx is lower due to the low-pass filter used before envelope detection and the filters added in both receiver models. However, using SNR referred at 20 MHz allows us to compare the results of the WuR modulations with standard WLAN signals.

The Peak-Flat modulation presented in this article was tested using both detector designs. Then, to get a more comprehensive idea of the Peak-Flat modulation performance, other state-of-the-art modulations used in WuR systems are also examined. For these modulations, the OOK receiver defined in Section VIII-B was used as a reference receiver. The modulations tested were: an OOK modulation at 250 kbps and the IEEE 802.11ba fast data rate modulation. All of them were tested using ideal square pulses.

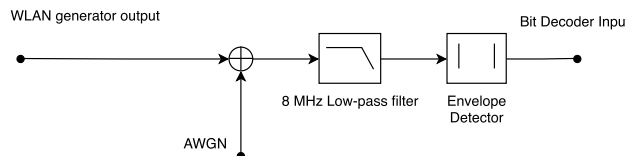


FIGURE 17. Diagram of the signal processing chain used for AWGN BER simulation.

The signal processing chain used in the AWGN based BER test is shown in Fig.17. It is based on the WuRx structure proposed in Section VIII-A and displayed in Fig.14. The AWGN is added at the start of the simulation chain. Then, the received signal, plus the noise are filtered and demodulated using an ideal envelope detector. Finally, the resulting signal is input to the Bit Decoder. The results from the Bit Decoder are sampled and compared with the input bit stream for BER computation. The AWGN simulation is performed in steps of $0.5\ \text{dB}$ of SNR. For each simulation step, 64000 bits are used to calculate the BER.

AWGN simulation results are shown in Fig.19a, for BER values down to $5 \cdot 10^{-4}$. Peak-Flat modulation, evaluated with the peak detector, achieves a 10^{-3} BER at roughly $3.5\ \text{dB}$ of SNR, whereas IEEE 802.11ba needs at least $4.5\ \text{dB}$ SNR to achieve the same result. OOK falls behind at roughly $5\ \text{dB}$ SNR for a sensitivity of 10^{-3} and, finally, Peak-Flat

modulation, decoded with OOK detector, falls well behind the other options, at $12.5\ \text{dB}$.

The TGn Ch.B simulation signal processing chain used to simulate PER results in fading channels is shown in Fig. 18. In contrast to the prior AWGN simulation, now the incoming WLAN signal is distorted by a fading channel based in TGn Channel B model. This simulation is executed in steps of $0.5\ \text{dB}$, with 5000 frames simulated per step.

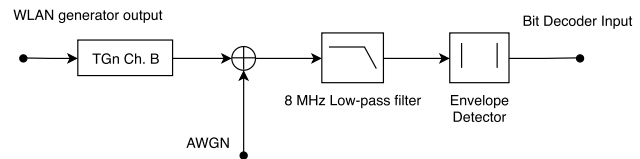


FIGURE 18. Diagram of the signal processing chain used for TGn Ch.B PER simulation.

Fading channel simulation results are shown in Fig.19b, for PER values down to $5 \cdot 10^{-2}$, evaluated with frames 128 bits long and ideal sampling times. Peak-Flat modulation, evaluated with the peak detector, achieves a 10^{-1} PER at $10\ \text{dB}$ of SNR, IEEE 802.11ba and OOK achieve the same result at $13\ \text{dB}$ SNR. Finally, Peak-Flat modulation, decoded with OOK detector, falls behind the other options, at $19\ \text{dB}$.

Thus, the Peak-Flat modulation performance appears to be better, in comparison with the current state-of-the-art modulations when tested with the proposed WuRx implementations. However, more complex and specialized IEEE 802.11ba receivers can achieve better results than the receivers proposed in this paper, which were designed with the aim to provide equitable demonstration platforms. In this way, preliminary results appearing in several TGba documents already suggest that better sensitivity figures are achievable for IEEE 802.11ba [20], [21]. Moreover, the Peak-Flat modulation receiver can be evolved from the PoC receiver presented in this paper into a more advanced one. Additionally Peak-Flat modulation provides the added value of being compatible with legacy IEEE 802.11 equipment while maintaining coexistence with current WLAN communications.

IX. COMPATIBILITY WITH IEEE 802.11ba

IEEE 802.11ba and the WuR system proposed in this paper use amplitude-based modulations that can be received with OOK detectors. This fact opens the possibility of interoperability between the two WuR systems. Nonetheless, due to the different modulations used in each system, the resulting interoperability is not straightforward.

Our system, which uses Peak-Flat modulated signals, sends and receives $4\ \mu\text{s}$ -long pulses that are physically compatible with the slower mode defined by IEEE 802.11ba: IEEE 802.11ba Low Rate (LR). This mode uses 4 pulses, each $4\ \mu\text{s}$ long, to encode one bit, thus, achieving a bit rate of 62.5 Kbps. A Peak-Flat WuTx can create a LR IEEE 802.11ba PHY symbol by concatenating 4 Peak-Flat symbols.

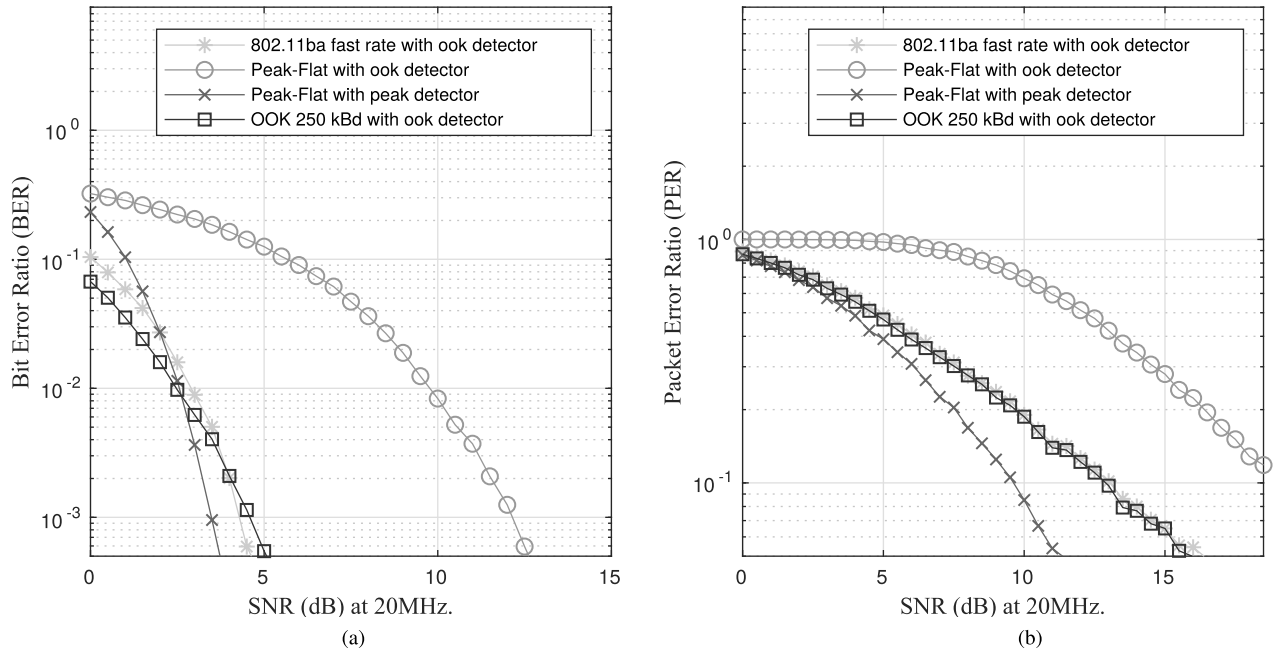


FIGURE 19. Simulation of Peak-Flat performance on the presented receivers versus various modulations. (a) BER vs SNR in AWGN channel. (b) PER vs SNR in TGn Ch.B.

There are then two possible interactions between devices implementing our Peak-Flat based WuR solution and IEEE 802.11ba devices.

- **IEEE 802.11ba as WuTx, Peak-Flat as WuRx:**

As discussed in Section VIII, the WuRx for the Peak-Flat device can be implemented using two different architectures. If the OOK detector architecture is used, then, the LR IEEE 802.11ba WuS signal will be detected since it is already OOK-coded. However, the OOK-coded signal cannot be reliably decoded by the peak detector design due to its higher detection threshold, that misses most ‘1’ OOK pulses.

- **Peak-Flat as WuTx, IEEE 802.11ba as WuRx:**

Even if the data symbols are electrically compatible, synchronization still has to be considered. The current draft of IEEE 802.11ba defines a synchronization preamble composed by a number of pulses with a duration of $2\mu s$ each. Currently, the generation of such pulses is not possible with Peak-Flat. As a consequence, the WuR system described in this paper is not currently compatible with IEEE 802.11ba in transmission, i.e., frames generated with Peak-Flat will not be detected by IEEE 802.11ba stations.

X. CONCLUSIONS AND FUTURE WORK

We devised a complete WuR system, as an alternative to IEEE 802.11ba, that is compatible with legacy IEEE 802.11 transmitters. The WuTx for this system is based on a standard compliant IEEE 802.11 OFDM PHY, for which a PoC has been presented using IEEE 802.11g. The signal modulation scheme of this WuR system, called Peak-Flat,

uses signal amplitude for signaling and can be decoded using low-power receivers such as those based on envelope detectors. The proposed Peak-Flat modulation used by the WuTx can be generated by any given IEEE 802.11 OFDM PHY transmitter, as long as its scrambler seed can be known in advance. At the moment of writing this paper, support for this feature is not found on most common IEEE 802.11 chipset drivers, however, we believe that the possibility of using WuR with them will drive more manufacturers to expose this functionality at the driver level or, alternatively, document the seed generation procedure so the scrambler seed can be effectively predicted. Two alternative WuRx designs for the proposed WuTx have been presented. The performance of the Peak-Flat modulation has been evaluated with the designed WuRx, and compared, using the same receiver designs, to other state-of-the-art WuR modulations such as an ideal OOK and the IEEE 802.11ba proposal. The resulting Peak-Flat modulation performance achieves better sensitivities with AWGN using the proposed receivers and more notable improvements using a fading channel model.

As part of our future work, we plan to apply the simulation results presented in this work to the implementation of a physical testbed for our WuR system. With that goal in mind, we propose to:

- 1) Implement the WuTx using the proposed software method with an IEEE 802.11 transceiver where the scrambler seed can be either predicted or directly read from the device.
- 2) Design and implement WuRx hardware prototype with both receiver architectures proposed: low-pass and peak detection.

- 3) Benchmark our legacy-compatible solution against IEEE 802.11ba compliant hardware on both range and power consumption.

REFERENCES

- [1] Wi-Fi Alliance. (2018). *Wi-Fi Gains Momentum in 2018*. Accessed: May 10, 2018. [Online]. Available: <https://www.wi-fi.org/beacon/the-beacon/wi-fi-gains-momentum-in-2018>
- [2] World Economic Forum. (2016). *Where is the World's Wi-Fi*. Accessed: May, 10, 2018. [Online]. Available: <https://www.weforum.org/agenda/2016/03/where-are-the-world-s-wifi-networks/>
- [3] V. Baños-Gonzalez, M. S. Afaqui, E. Lopez-Aguilera, and E. Garcia-Villegas, "IEEE 802.11 ah: A technology to face the IoT challenge," *Sensors*, vol. 16, no. 11, p. 1960, 2016.
- [4] M. Tauber and S. N. Bhatti, "The effect of the 802.11 power save mechanism (PSM) on energy efficiency and performance during system activity," in *Proc. IEEE Int. Conf. Green Comput. Commun. (GreenCom)*, Nov. 2012, pp. 573–580.
- [5] J. Oller, I. Demirkol, J. Casademont, J. Paradells, G. U. Gamm, and L. Reindl, "Wake-up radio as an energy-efficient alternative to conventional wireless sensor networks MAC protocols," in *Proc. 16th ACM Int. Conf. Modeling, Anal. Simulation Wireless Mobile Syst. (MSWiM)*, New York, NY, USA, 2013, pp. 173–180. [Online]. Available: <http://doi.acm.org.recursos.biblioteca.upc.edu/10.1145/2507924.2507955>
- [6] J. Oller et al., "Has time come to switch from duty-cycled MAC protocols to wake-up radio for wireless sensor networks?" *IEEE/ACM Trans. Netw.*, vol. 24, no. 2, pp. 674–687, Apr. 2016.
- [7] *Proposal for Wake-Up Receiver (WUR) Study Group*. Standard IEEE 802.11 TGba, 2016, Accessed: May 10, 2018. [Online]. Available: <https://mentor.ieee.org/802.11/dcn/16/11-16-0722-01-0000-proposal-for-wake-up-receiver-study-group.pptx>
- [8] R. Piyare, A. L. Murphy, C. Kiraly, P. Tosato, and D. Brunelli, "Ultra low power wake-up radios: A hardware and networking survey," *IEEE Commun. Surveys Tuts.*, vol. 19, no. 4, pp. 2117–2157, 4th Quart., 2017.
- [9] The MathWorks. (2018). *Reference Web-Page for MATLAB WLAN Toolbox*. Accessed: Jun. 5, 2018. [Online]. Available: <https://es.mathworks.com/help/wlan/>
- [10] The MathWorks. (2018). *Simscape Electronics Reference Web-Page*. Accessed: Jun. 21, 2018. [Online]. Available: <https://www.mathworks.com/products/simelectronics.html>
- [11] E.-Y. A. Lin, J. M. Rabaey, and A. Wolisz, "Power-efficient rendez-vous schemes for dense wireless sensor networks," in *Proc. IEEE Int. Conf. Commun.*, vol. 7. Jun. 2004, pp. 3769–3776.
- [12] A. Dunkels, "The contikimac radio duty cycling protocol," SICS (Swedish ICT), Stockholm, Sweden, Tech. Rep. T2011:13, 2011.
- [13] H. Zhang, C. Li, S. Chen, X. Tan, N. Yan, and H. Min, "A low-power OFDM-based wake-up mechanism for IoE applications," *IEEE Trans. Circuits Syst. II, Exp. Briefs*, vol. 65, no. 2, pp. 181–185, Feb. 2018.
- [14] J. Oller et al., "IEEE 802.11-enabled wake-up radio system: Design and performance evaluation," *Electron. Lett.*, vol. 50, no. 20, pp. 1484–1486, 2014.
- [15] Y. Kondo et al., "Wake-up radio using IEEE 802.11 frame length modulation for radio-on-demand wireless LAN," in *Proc. IEEE 22nd Int. Symp. Pers., Indoor Mobile Radio Commun.*, Sep. 2011, pp. 869–873.
- [16] As3933 LF Receiver IC. Accessed: Sep. 16, 2018. [Online]. Available: <https://ams.com/as3933>
- [17] E. Park, D. Lim, J. Chun, and Choi. (2018). *OOK Waveform Generation*. Accessed: Jun. 10, 2018. [Online]. Available: <https://mentor.ieee.org/802.11/dcn/18/11-18-0072-00-00ba-ook-waveform-generation.pptx>
- [18] S. Shellhammer and R. Yang. (2018). *MC-OOK on Symbol Generation*. Accessed: Jun. 10, 2018. [Online]. Available: <https://mentor.ieee.org/802.11/dcn/18/11-18-0584-03-00ba-on-symbol-generation.pptx>
- [19] *IEEE Standard for Information Technology—Telecommunications and Information Exchange Between Systems—Local and Metropolitan Area Networks—Specific Requirements—Part 11: Wireless LAN Medium Access Control (MAC) and Physical Layer (PHY) Specifications*, Standard IEEE 802.11-2007, Jun. 2007, pp. 1–1238
- [20] M. Lopez, D. Sundman, and L. Wilhelmsson. (2018). *MC-OOK Symbol Design*. Accessed: Sep. 14, 2018. [Online]. Available: <https://mentor.ieee.org/802.11/dcn/18/11-18-0479-02-00ba-mc-ook-symbol-design.pptx>
- [21] V. Kristem, S. Azizi, and T. Kenney. *MC-OOK Symbol Design*. 2018. Accessed: Jun. 10, 2018. [Online]. Available: <https://mentor.ieee.org/802.11/dcn/18/11-18-0492-02-00ba-2us-ook-waveform-generation.pptx>
- [22] S. A. Talwalkar and S. L. Marple, "Time-frequency scaling property of discrete Fourier transform (DFT)," in *Proc. IEEE Int. Conf. Acoust., Speech Signal Process.*, Mar. 2010, pp. 3658–3661.
- [23] B. Bloessl, C. Sommer, F. Dressier, and D. Eckhoff, "The scrambler attack: A robust physical layer attack on location privacy in vehicular networks," in *Proc. Int. Conf. Comput., Netw. Commun. (ICNC)*, 2015, pp. 395–400.
- [24] *IEEE Standard for Information Technology—Local and Metropolitan Area Networks—Specific Requirements—Part 11: Wireless LAN Medium Access Control (MAC) and Physical Layer (PHY) Specifications Amendment 5: Enhancements for Higher Throughput*, Standard IEEE 802.11n-2009, Oct 2009, pp. 1–565.
- [25] *IEEE Standard for Information Technology—Telecommunications and Information Exchange Between Systems—Local and Metropolitan Area Networks—Specific Requirements—Part 11: Wireless LAN Medium Access Control (MAC) and Physical Layer (PHY) Specifications—Amendment 4: Enhancements for Very High Throughput for Operation in Bands Below 6 GHz*, Standard IEEE 802.11ac(TM)-2013, Dec 2013, pp. 1–425.



MARTÍ CERVIÀ CABALLÉ was born in Manresa, Barcelona, Spain, in 1992. He received the B.S. degree in telecommunications engineering and the M.Sc. degree in telecommunication engineering from the Universitat Politècnica de Catalunya (UPC), in 2015 and 2017, respectively, where he is currently pursuing the Ph.D. degree in network engineering. His areas of interests include wireless sensor networks, digital communications, and low-power transceiver design.



ANNA CALVERAS AUGÉ was born in Barcelona, Spain, in 1969. She received the Ph.D. degree in telecommunications engineering from the Universitat Politècnica de Catalunya, Spain, in 2000, where she is currently an Associate Professor with the Wireless Networks Group (WNG), Department of Network Engineering. Her research interests and expertise areas comprise the design, evaluation, and optimization of communications protocols and architectures for cellular, wireless multihop networks, ad-hoc networks, wireless sensor networks, the Internet of Things, and application domains such as smart cities, building automation, and emergency environments. She has been involved in several National and International research or technology transfer projects, and has published in International and National conferences and journals.



ELENA LOPEZ-AGUILERA received the M.Sc. degree in telecommunications engineering from the Universitat Politècnica de Catalunya (UPC), in 2001, and the Ph.D. degree from UPC, in 2008, where she is currently an Associate Professor and a member of the Wireless Networks Group (WNG), Department of Network Engineering. Her main research interests include the study of IEEE 802.11 WLANs and the Internet of Things enabling technologies in heterogeneous scenarios. Her experience comprises QoS, security, radio resource management, location mechanisms, and wake-up radio systems. She has published papers in journals and conferences in the area of wireless communications and has been involved in projects with public and private funding.



EDUARD GARCIA-VILLEGAS is currently an Associate Professor with the Universitat Politècnica de Catalunya (UPC), and a member of the Wireless Networks Group (WNG). He participates in the activities of the IEEE P802.11 WG and in the research developed within the i2CAT Foundation. After being awarded a José Castillejo Grant for young doctors, he collaborates with the MOMENT Lab, UC Santa Barbara. His research interests include the IEEE 802.11 WLANs, radio resource management in wireless networks, and the Internet of Things enabling technologies (sensor networks, mesh, and multi-hop ad-hoc networks).



JOSEP PARADELLS ASPAS is currently the Director of the Fundació i2CAT and a Professor with the Universitat Politècnica de Catalunya (UPC). He is also the Co-Director of the master's program in the IoT offered by Fundació UPC. He has been working in the area of Internet of Things, in particular with wireless interfaces and protocols. He has participated in national and European public-funded research projects and collaborated with several Spanish telecommunications companies. In 2012, he was recognized as the Best Academic Trajectory.



İLKER DEMIRKOL received the B.S., M.S., and Ph.D. degrees in computer engineering from Bogazici University, Istanbul, Turkey. He is currently a Ramon y Cajal Research Professor with the Department of Network Engineering, Universitat Politècnica de Catalunya. His research focus is on communication protocol development and performance evaluation of wireless networks. He has held several positions both in academia and industry, such as network engineer, system, and database consultant. He is a recipient of the Best Paper Award in the IEEE ICC 2013, and the Best Mentor Award at the University of Rochester, NY, USA, in 2010.